HELLENIC REPUBLIC
National and Kapodistrian
University of Athens
EST. 1837

ALICE

Resonance production from pp to heavy-ion collisions

Paraskevi Ganoti
National and Kapodistrian University of Athens (GR)

Particle physics seminar, University of Birmingham
20 October 2021

Outline

- **Heavy-ion physics - main concepts**
- **Hadronic resonances - physics motivation**
- **Hadronic resonances - results from ALICE (mainly)**
  - p_T spectra in pp, p–Pb and heavy-ion collisions.
  - p_T integrated yields and $\langle p_T \rangle$.
  - Particle yield ratios.
  - Nuclear modification factors.
- **The future of hadronic resonances and summary**

Heavy-ion Physics

- **Study matter**
  - At energy densities like 10 μs after the Big Bang.
  - At temperatures 10^5 times larger than in the Sun core.
- **Study QCD**
  - Without confinement.
  - With quarks at their bare masses.
- **But also:**
  - Study QCD in the non-perturbative regime.

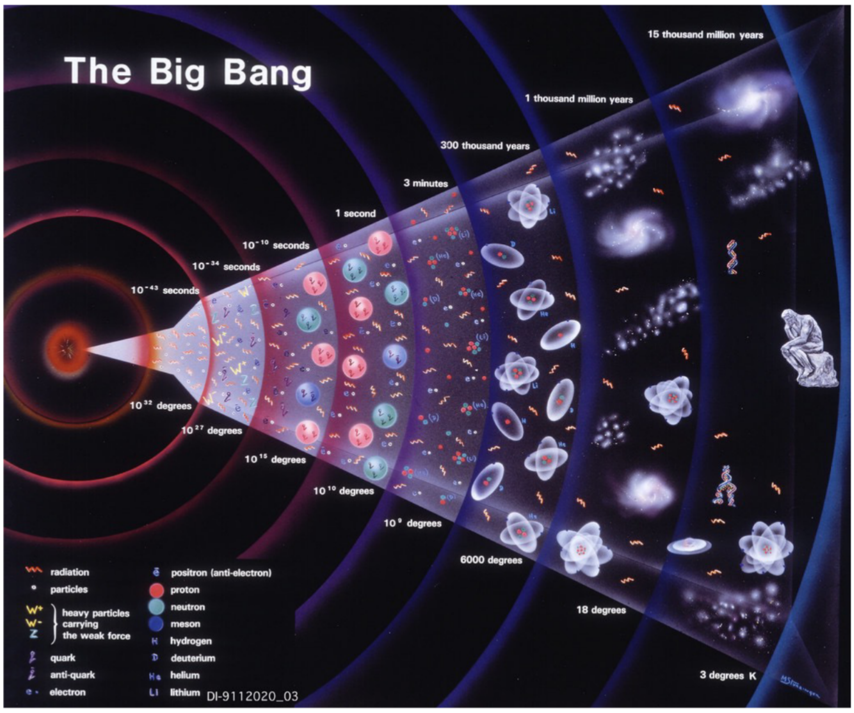

Heavy-ion Physics

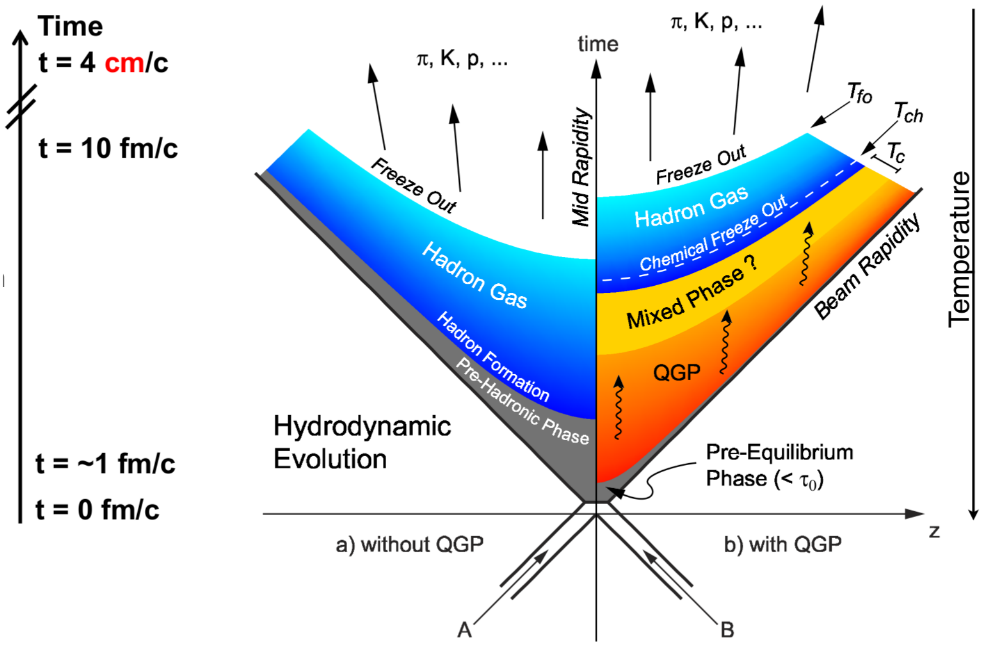

- ❖ Kinetic freeze-out
  - Elastic reactions cease: p_T spectra (free streaming of hadrons)
- ❖ Chemical freeze-out
  - Inelastic reactions cease: The chemical composition of the system is fixed (particle yields)
- ❖ Phase transition from QGP to hadron gas
  - Formation of Quark-Gluon Plasma phase (if $T > T_C$)
- ❖ "Pre-equilibrium"
- ❖ Two Lorentz contracted nuclei approach and collide

Heavy-ion Physics

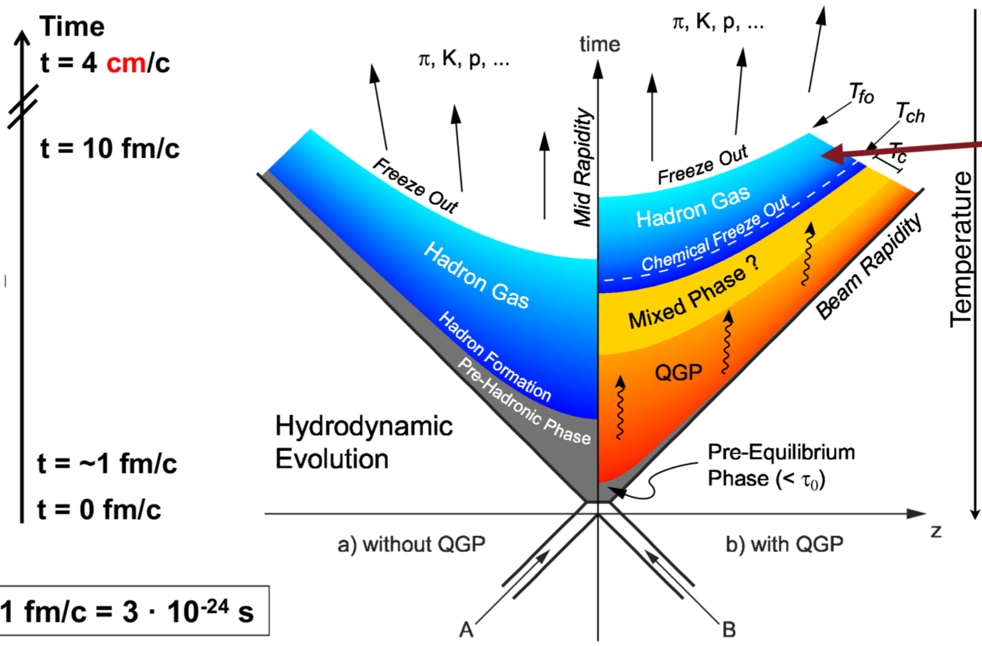

1 fm/c = 3 · 10^{-24} s

Region accessible through resonance measurements.

QCD Phase Diagram

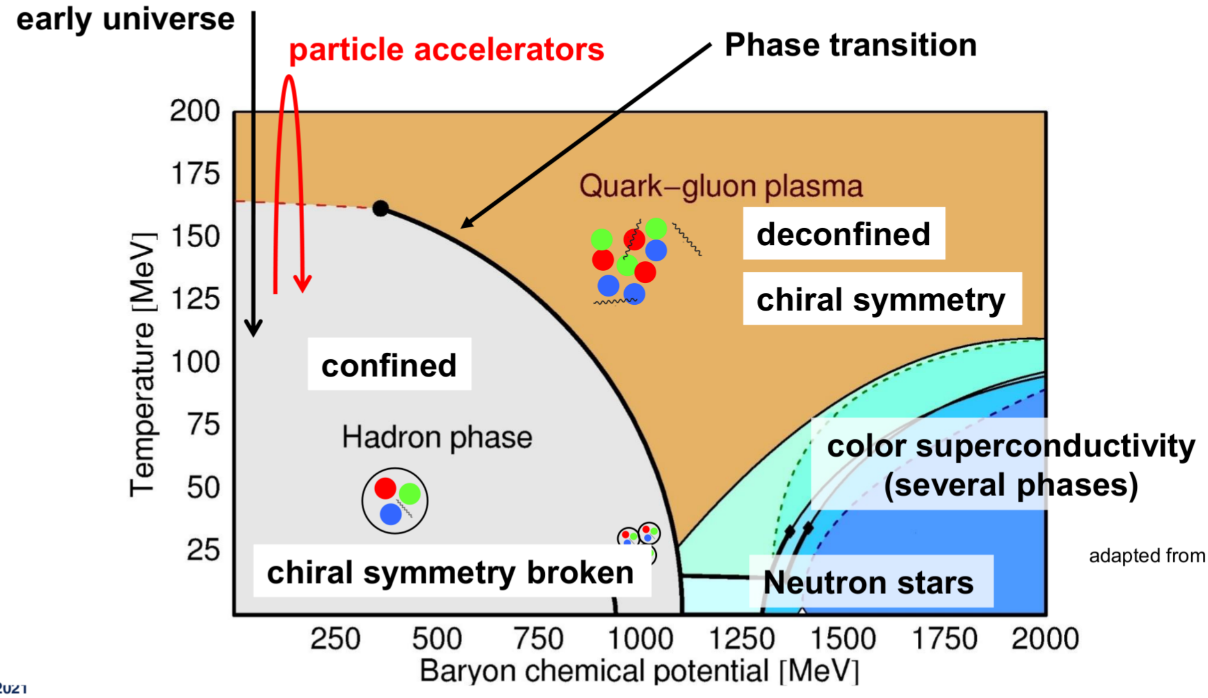

adapted from hep-ph/0503184

The ALICE detector

- Inner Tracking System (ITS)
  - 6 layers of silicon detectors
  - Provide trigger, tracking, vertex, PID (dE/dx)

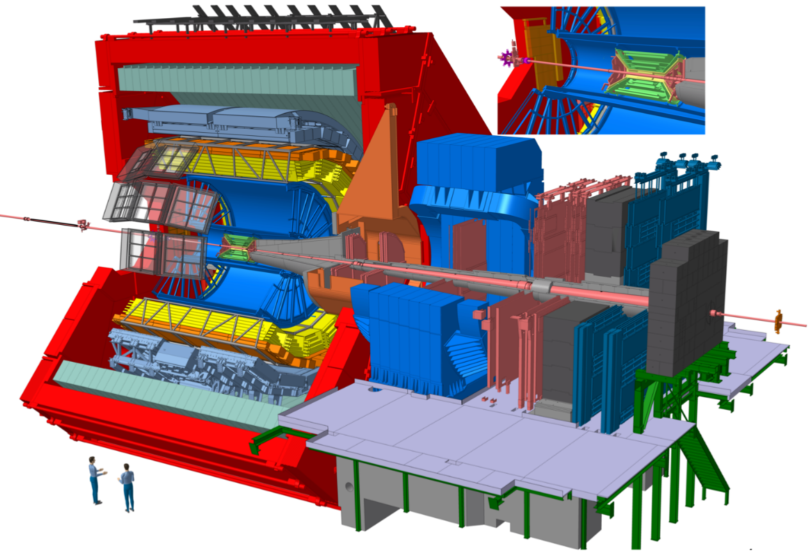

- Time Projection Chamber (TPC)
  - Gas-filled ionization detector
  - Tracking, vertex, PID (dE/dx)
- Time Of Flight (TOF)
  - PID through particle time of flight
- V0A and V0C
  - Trigger, centrality/multiplicity estimator

System	Year	$\sqrt{s_{NN}}$ (TeV)
Pb–Pb	2010 2011 2015 2018	2.76 2.76 5.02 5.02
Xe–Xe	2017	5.44
p–Pb	2013 2016	5.02 5.02, 8.16
pp	2009-2013 2015-2018	0.9, 2.76, 7 8, 13

Geometry and centrality of the collision

Geometry of a heavy-ion collision

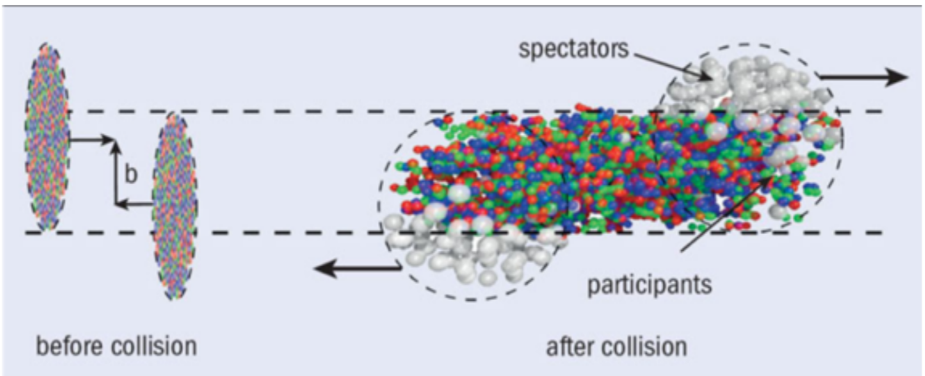

b: impact parameter.

b=**0-5 fm**: 0-10% **central** collisions
b=**10-12 fm**: 60-80% **peripheral** collisions.

Geometry and centrality of the collision

Glauber Monte Carlo:

Input: nuclear charge densities.
inelastic nucleon-nucleon cross section.

Assumptions:

- **Nucleons travel on straight lines**
- **Collisions do not alter their trajectory (energy of nucleons large enough)**
- **No quantum-mechanical interference**
- **Interaction probability for two nucleons is nucleon-nucleon cross-section**

Output:

- **Number of spectators (nucleons that do not collide).**
- **Participant or wounded nucleons (N_{part}).**
- **Number of binary collisions (N_{coll}).**

Blue nucleon has suffered 5 NN collisions.

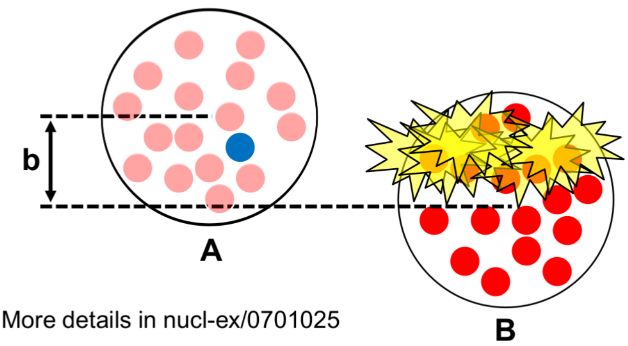

More details in nucl-ex/0701025

Geometry and centrality of the collision

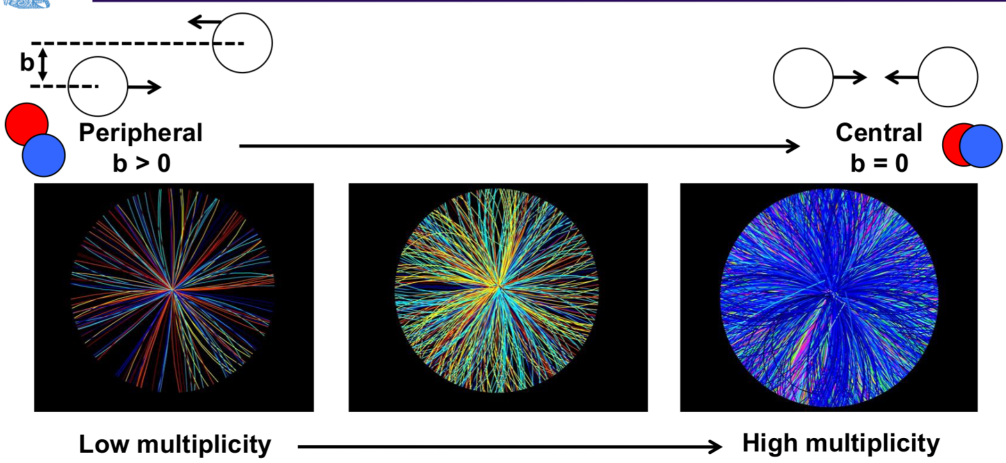

Multiplicity is anti-proportional to b.

Glauber MC + particle production model calculates multiplicity.

Multiplicity is calculated experimentally by detectors.

The experimental distribution is fitted with the one from the Glauber MC.
Events are split into classes, called 0–5%, 5–10% etc. The 0–5% class is the most central.

Geometry and centrality of the collision

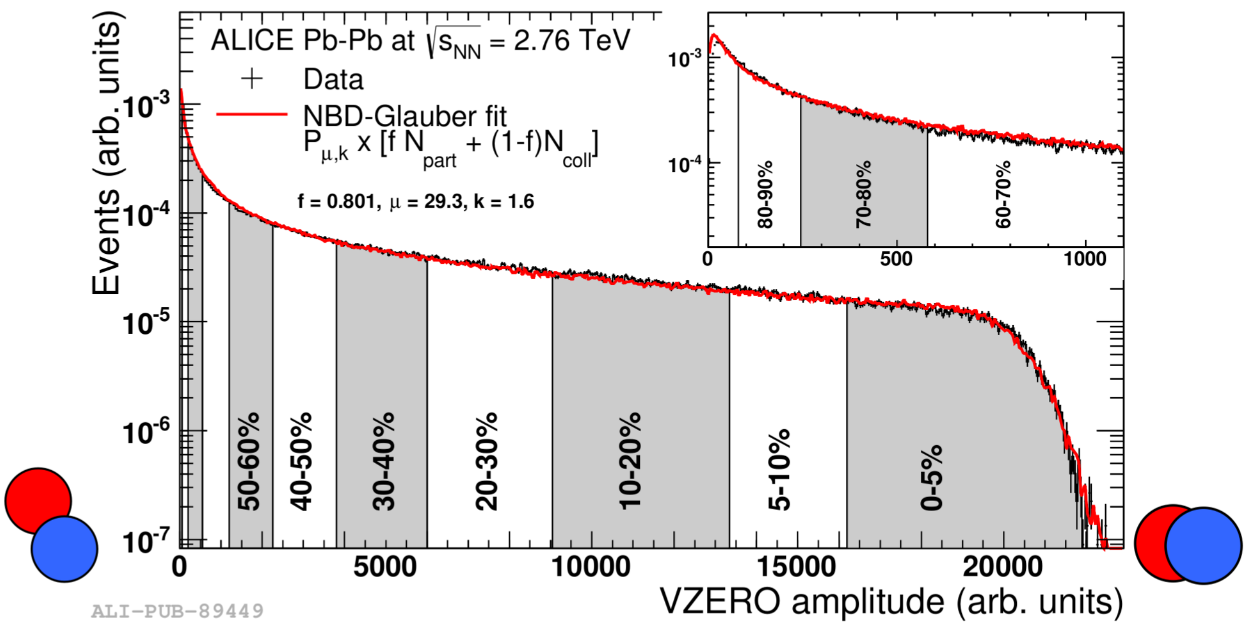

PHYSICAL REVIEW C 88, 044909 (2013)

Physics motivation

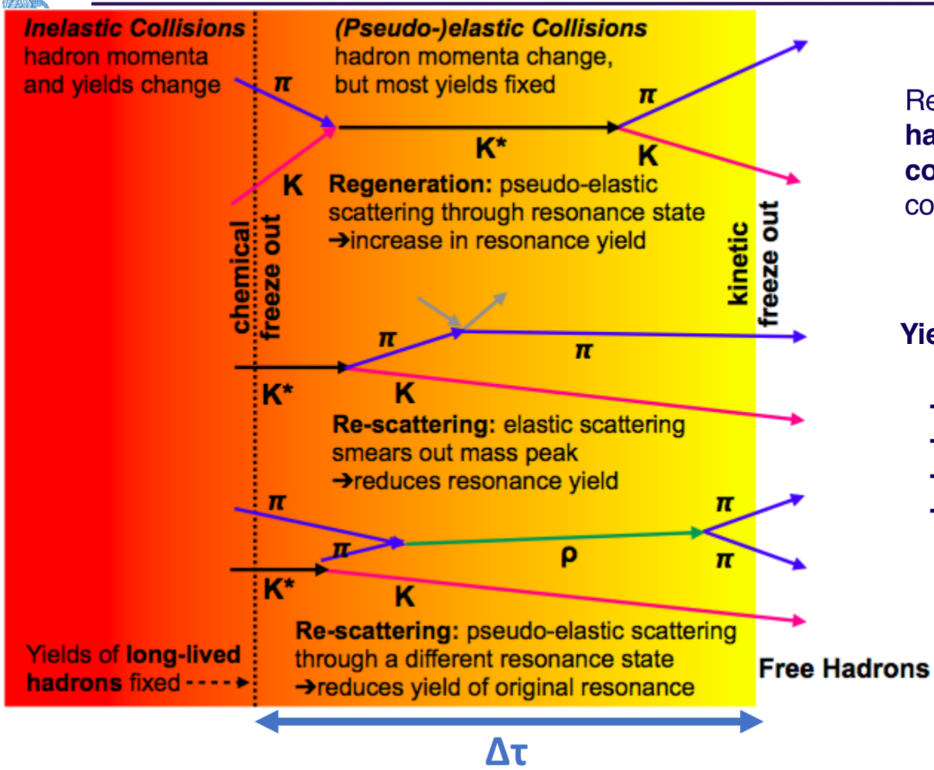

Resonances are ideal probes to study the **hadronic phase in nucleus - nucleus collisions,** as they have lifetimes comparable with the fireball lifetime.

Yields at kinetic freeze-out depend on:

- Resonance lifetime
- Lifetime of the hadronic phase (Δτ)
- Yield at the chemical freeze-out
- Scattering cross sections of decay products

Physics motivation

Resonance	$\rho(770)^0$	$K^*(892)^\pm$	$K^*(892)^0$	$f_0(980)$	$\Sigma(1385)^\pm$	$\Xi(1820)^\pm$	$\Lambda(1520)$	$\Xi(1530)^0$	$\phi(1020)$
Quark composition	$\frac{u\bar{u}+d\bar{d}}{\sqrt{2}}$	$u\bar{s}, \bar{u}s$	$d\bar{s}, \bar{d}s$	unknown	uus, dds	uss	uds	uss	$s\bar{s}$
τ(fm/c)	1.3	3.6	4.2	large unc.	5-5.5	8.1	12.6	21.7	46.4
Decay	$\pi\,\pi$	$K^0_s\,\pi$	$K\,\pi$	$\pi^+\pi^-$	$\Lambda\,\pi$	$\Lambda\,K$	$p\,K$	$\Xi\,\pi$	$K\,K$
B.R.(%)	100	33.3	66.6	46	87	unknown	22.5	66.7	48.9

Observables

Particle yields and ratios of identified particles	chemistry of the system and chemical freeze out temperature
p_T-differential spectra and ratios, mean p_T	system dynamics (radial flow, kinetic freeze out temperature)
System size scan	evolution with multiplicity of chemistry and dynamics (HIC like phenomena observed in high multiplicity pp and pA events)

Resonance reconstruction - Analysis strategy

- Resonances are reconstructed via the **invariant mass** technique.

$$M_{inv} = \sqrt{(E_1 + E_2)^2 - (\vec{p_1} + \vec{p_2})^2}$$

- **Uncorrelated background** is calculated via **event mixing or like-sign techniques**.
- **PID** from ITS, TPC, TOF for the **daughter tracks**.
- **Residual background**: Correlated pairs or misidentified decay products, usually modelled by a polynomial function.
- **Signal** : Fit the event-mixing (or like-sign) subtracted distribution with a Breit-Wigner or Voigtian function (signal function) and the polynomial background.
- Yields are calculated by integrating the signal function.

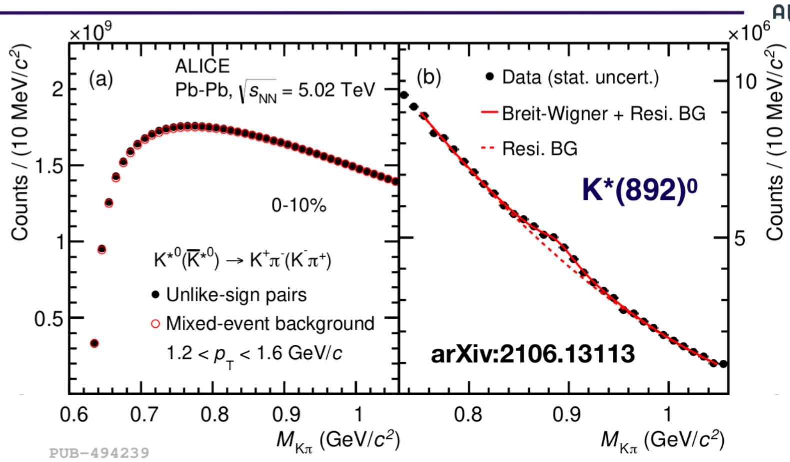

Resonance reconstruction - Analysis strategy

- Resonances are reconstructed via the **invariant mass** technique.

$$M_{inv} = \sqrt{(E_1 + E_2)^2 - (\vec{p_1} + \vec{p_2})^2}$$

- **Uncorrelated background** is calculated via **event mixing or like-sign techniques**.
- **PID** from ITS, TPC, TOF for the **daughter tracks**.
- **Residual background**: Correlated pairs or misidentified decay products, usually modelled by a polynomial function.
- **Signal** : Fit the event-mixing (or like-sign) subtracted distribution with a Breit-Wigner or Voigtian function (signal function) and the polynomial background.
- Yields are calculated by integrating the signal function.

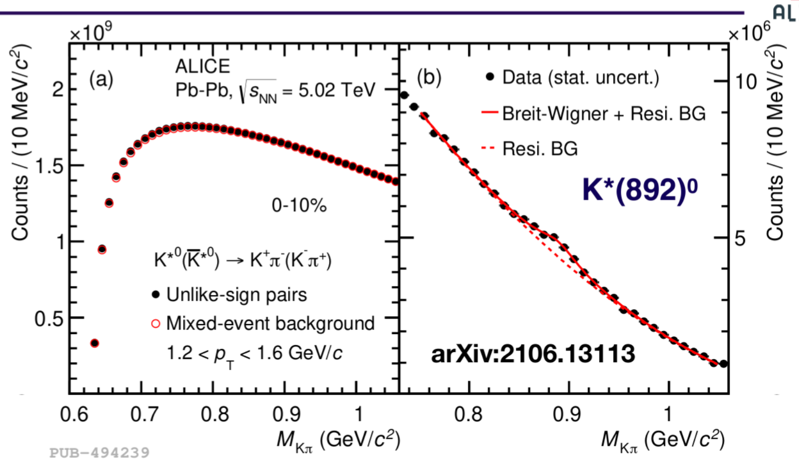

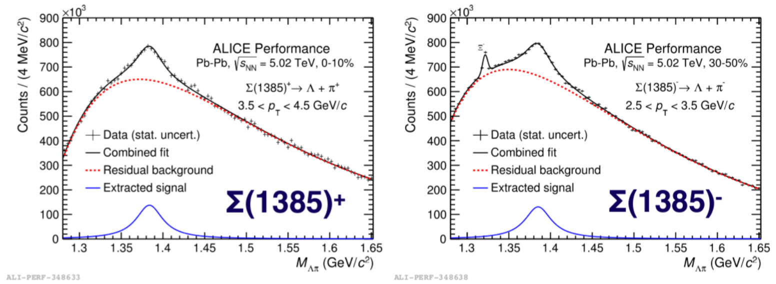

p_T spectra in heavy-ion collisions

ALICE has measured resonances in **Pb–Pb** collisions at $\sqrt{s_{NN}}$ = **2.76 TeV** and **5.02 TeV (**but also in **Xe–Xe** collisions at $\sqrt{s_{NN}}$ **= 5.44 TeV**).

ρ⁰

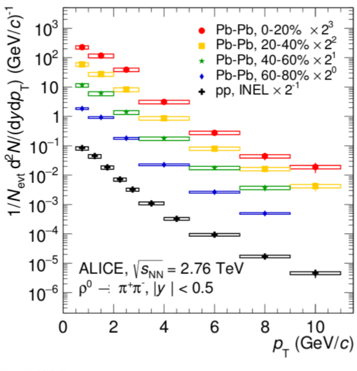

Phys.Rev. C99 (2019) 064901

Λ(1520)

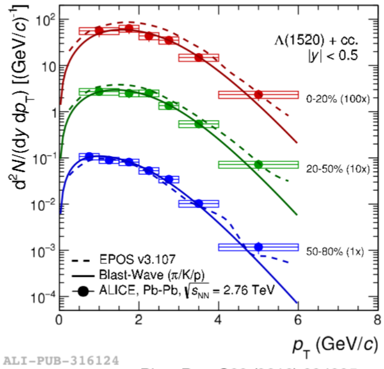

Phys.Rev. C99 (2019) 024905

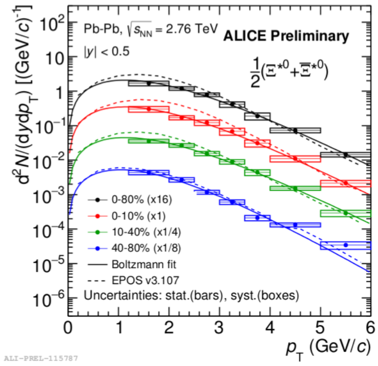

Ξ*0

p_T spectra in heavy-ion collisions

ALICE has measured resonances in **Pb–Pb** collisions at $\sqrt{s_{NN}}$ = **2.76 TeV** and **5.02 TeV (**but also in **Xe–Xe** collisions at $\sqrt{s_{NN}}$ **= 5.44 TeV**).

ρ⁰

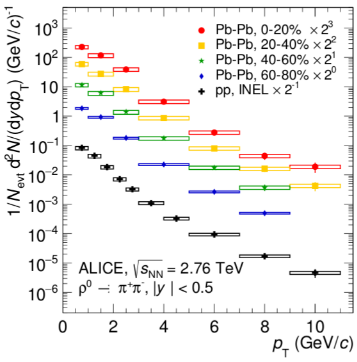

ALI-PUB-161346

Phys.Rev. C99 (2019) 064901

Λ(1520)

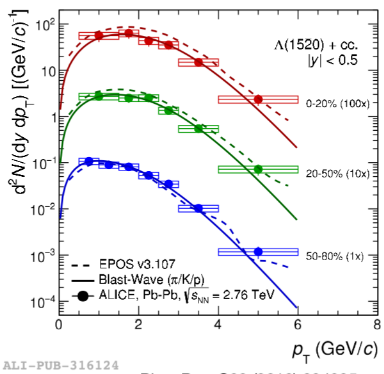

ALI-PUB-316124

Phys.Rev. C99 (2019) 024905

Ξ*⁰

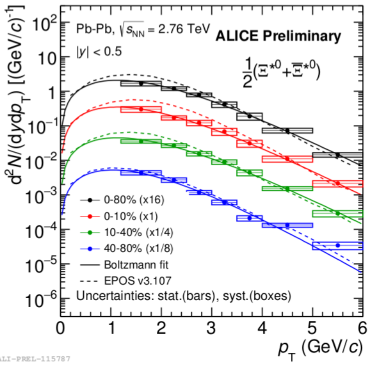

ALI-PREL-115787

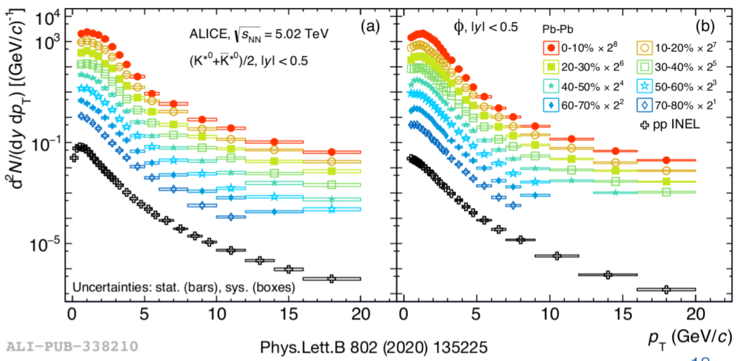

ALI-PUB-338210

Phys.Lett.B 802 (2020) 135225

Hardening of the spectra with increasing multiplicity
→caused by radial flow.

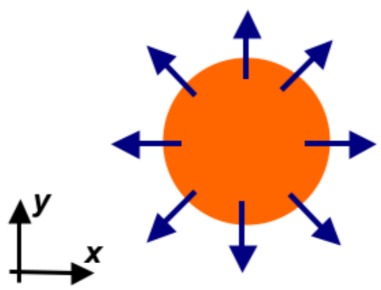

Radial flow: predicted by hydronamics in A–A due to the higher energy density.

- The only type of collective flow in A–A collisions with impact parameter b = 0.
- Affects the shape of particle spectra at low p_T.

p=mβγ

Common velocity field ***βγ*** fixed → **mass** dependence

p_T spectra in p–Pb collisions

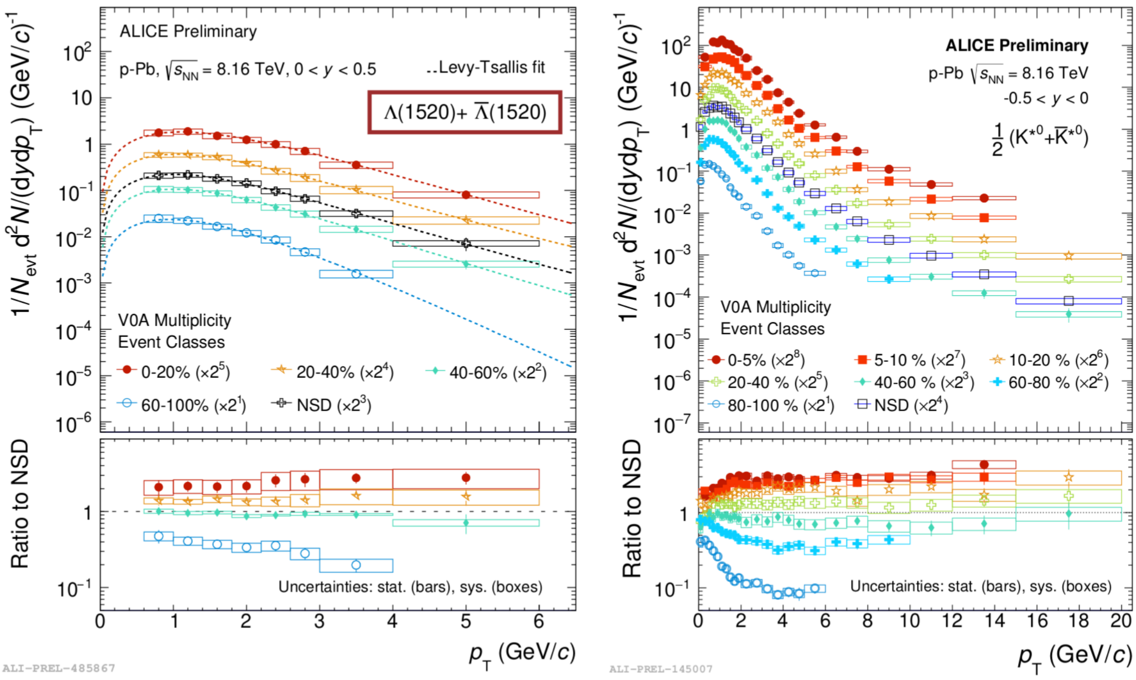

Qualitatively **similar observations** as for **heavy-ion collisions** regarding the **shapes**.

Collective flow-like effects in small collision systems.

p_T spectra in pp collisions

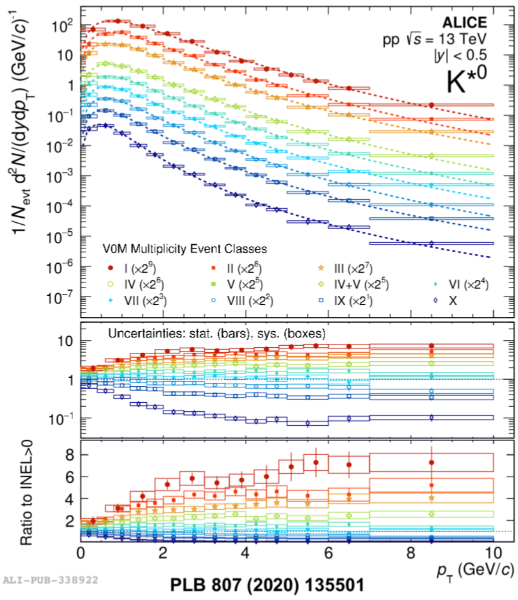

PLB 807 (2020) 135501

The **spectra shapes change with multiplicity** in the **same way** as for the **larger systems**.

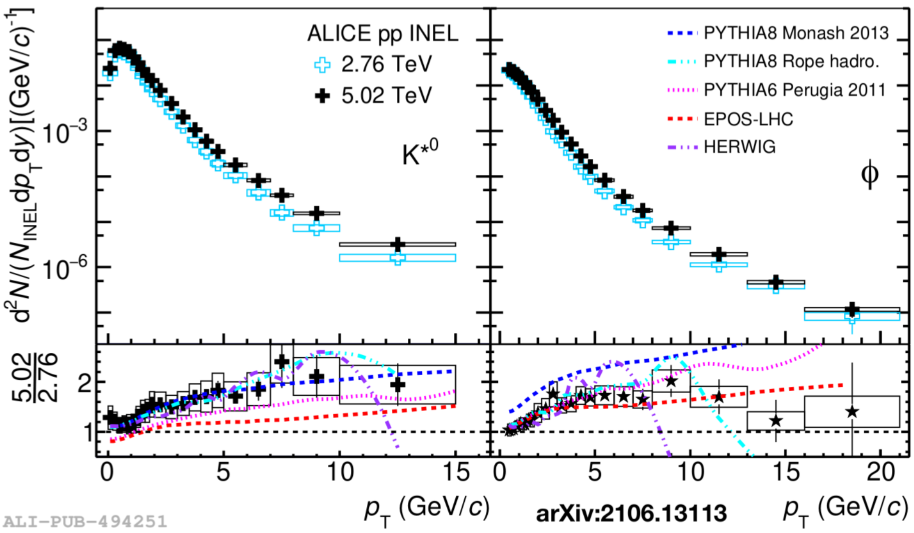

arXiv:2106.13113

Ratio between the two energies evolves with p_T.
Hint of **saturation at p_T ~ 5 GeV/*c*.**

Pythia tunes give good description except the Monash tune for the ϕ.
HERWIG describes the ratio for K* but ϕ only up to ~ 3 GeV/*c*.
EPOS-LHC underestimates K* but describes ϕ up to ~ 7-8 GeV/*c*.

p_T integrated yields

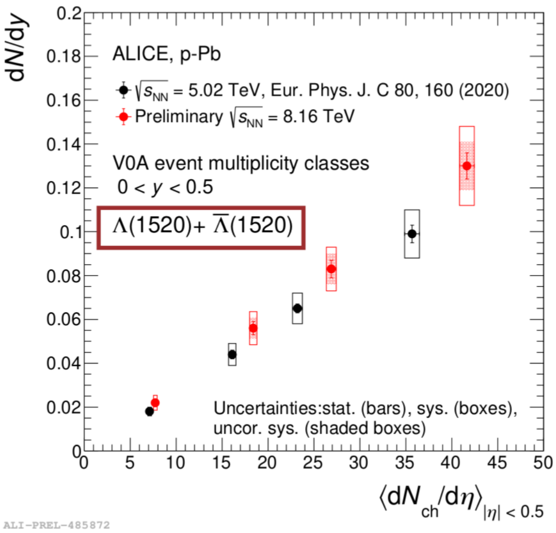

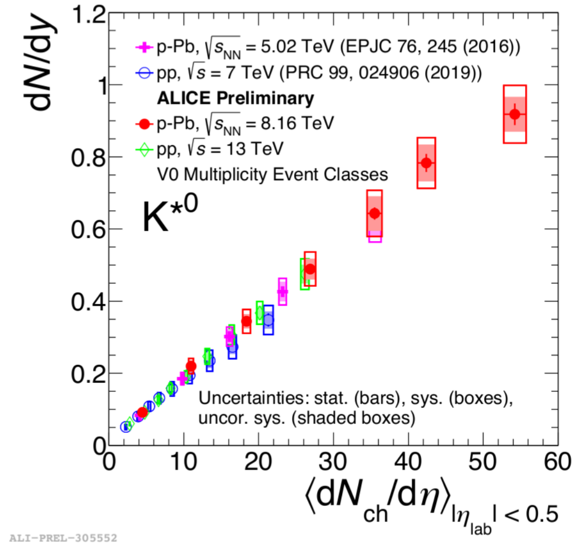

In pp and p–Pb collisions there is a linear increase of d*N*/d*y* following a common trend for all resonances analysed, independent of the collision system and energy.
Similar results are seen for strange hadrons.

p_T integrated yields

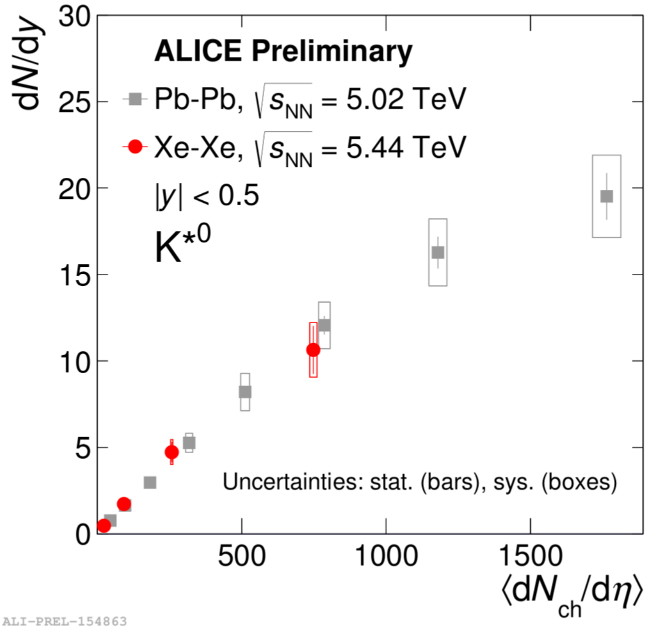

In heavy-ion collisions, **K^{*0}** production is driven by the multiplicity.

p_T integrated yields

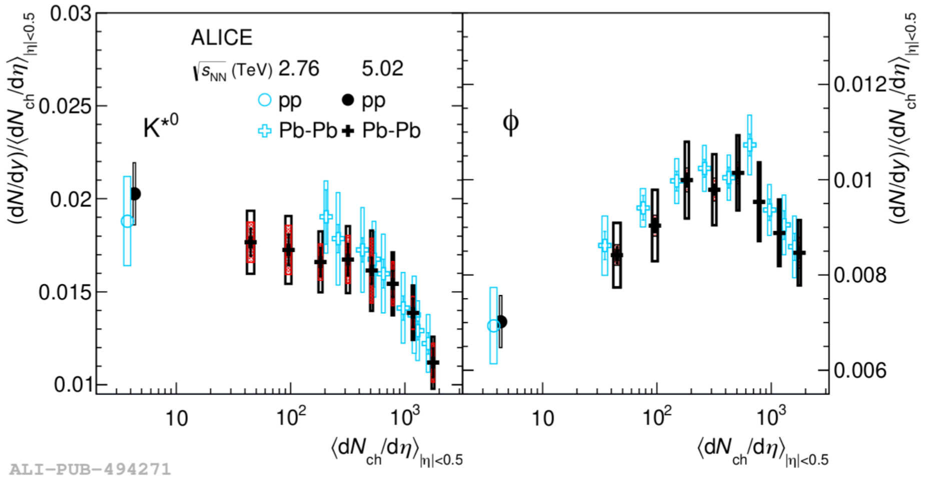

arXiv:2106.13113

dN/dy, scaled by the average charged particle multiplicity measured at midrapidity.

The dependence on ⟨dNch/dη⟩$_{|\eta|<0.5}$ is found to be the **same regardless of the beam energy.**

Mean transverse momentum

Phys. Lett. B 807 135501 (2020)

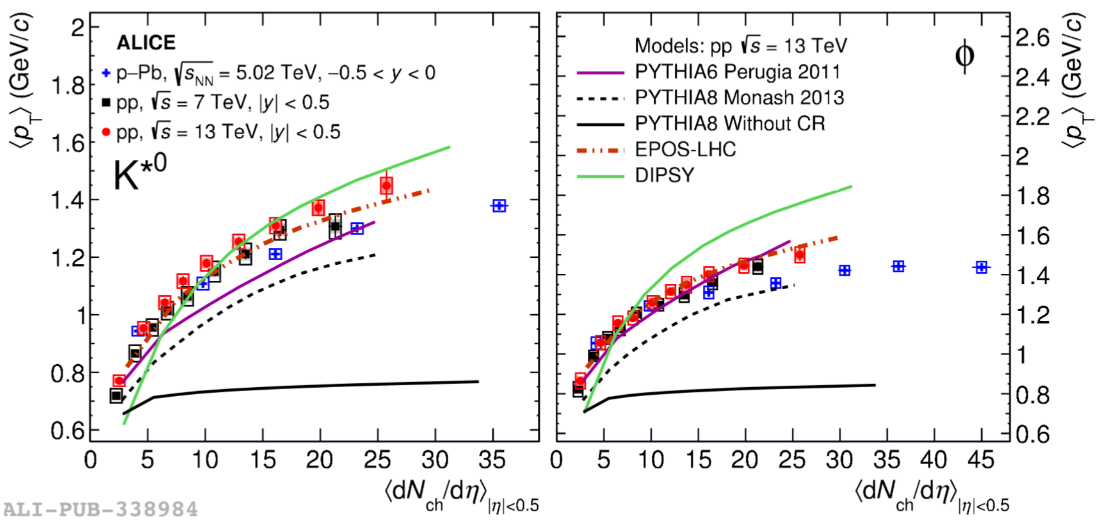

The ⟨$\boldsymbol{p_T}$⟩ values of K*0 and ϕ in pp collisions at **√s = 7 TeV and 13 TeV** follow approximately the same trend.

The ⟨$\boldsymbol{p_T}$⟩ values K*0 and ϕ **rise slightly faster** as a function of ⟨dN_{ch}/dη⟩$_{|\eta|<0.5}$ in **pp** collisions **than** in **p–Pb** collisions for ⟨dN_{ch}/dη⟩$_{|\eta|<0.5}$.

Mean transverse momentum

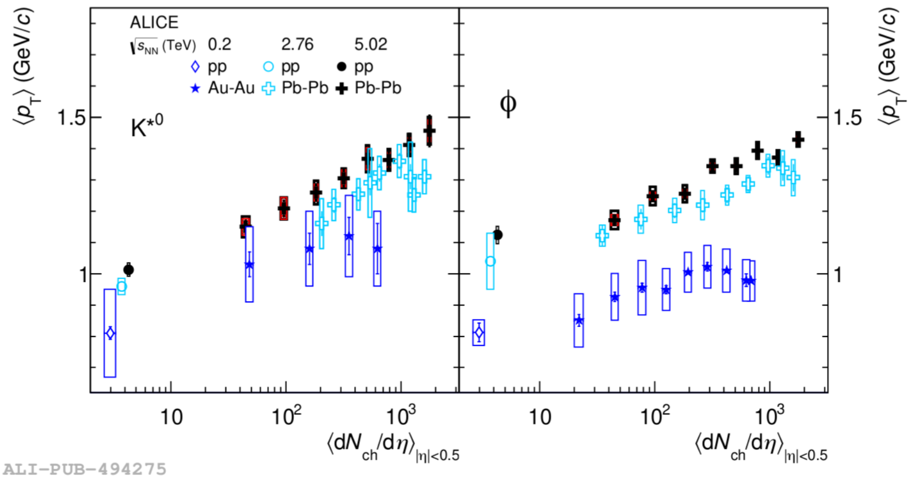

arXiv:2106.13113

The $\langle \boldsymbol{p}_T \rangle$ values increase with charged particle multiplicity.

The $\langle \boldsymbol{p}_T \rangle$ of K^{*0} and ϕ mesons (which have similar masses) are similar for events with the same $\langle dN_{ch}/d\eta \rangle_{|\eta|<0.5}$ in Pb–Pb collisions → Consistent with the picture of a growing contribution of radial flow with increasing $\langle dN_{ch}/d\eta \rangle_{|\eta|<0.5}$

The $\langle \boldsymbol{p}_T \rangle$ values are larger for higher energy collisions at similar values of $\langle dN_{ch}/d\eta \rangle_{|\eta|<0.5}$.

Mean transverse momentum

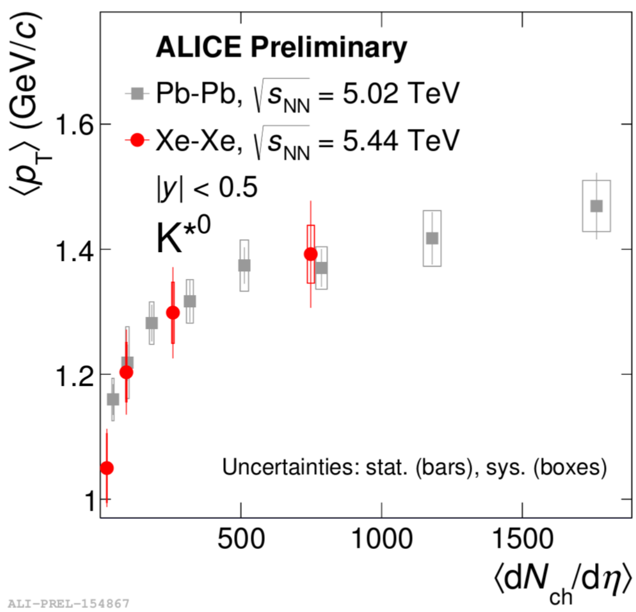

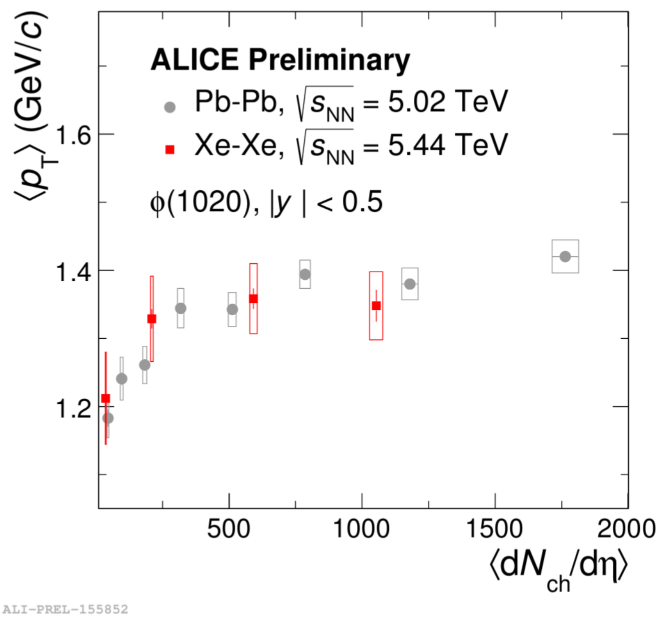

Similar evolution of $\langle p_T \rangle$ in **Pb–Pb** and **Xe–Xe** collisions.

Mean transverse momentum

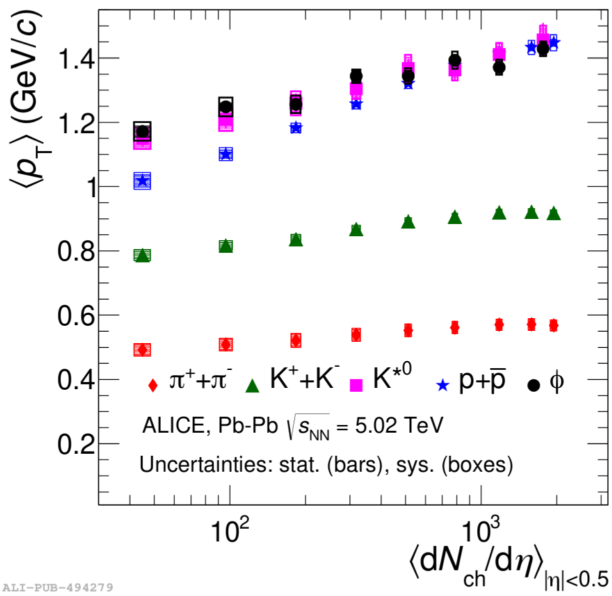

arXiv:2106.13113

Steeper rise of $\langle p_T \rangle$ for the heavier particles.

K*, p and **ϕ** (they have similar masses):

- At the higher multiplicities have similar $\langle p_T \rangle$ within the uncertainties.

- At lower multiplicities mass scaling is breaking.

Particle yield ratios

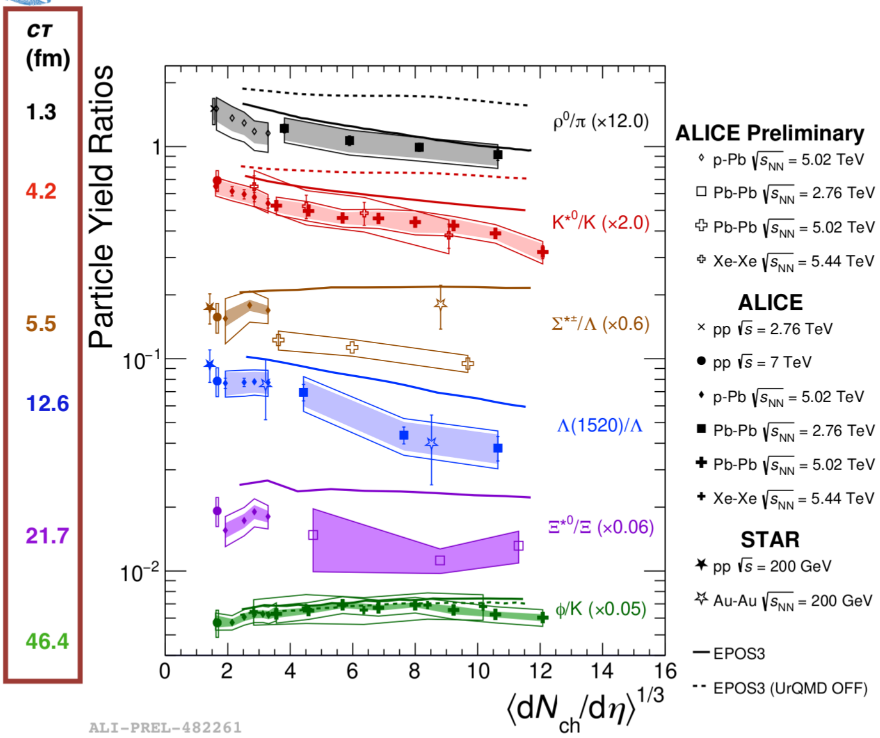

All particle ratios evolve smoothly with system size for the measured systems and energies.

Short-lived resonances like ρ⁰, K*⁰, Σ*± Λ* are affected by re-scattering in the hadronic phase.

Ξ* production is rather independent of the system size.

ϕ is not suppressed as it decays after the kinetic freeze-out.

EPOS with UrQMD qualitatively describes the trends, **except** for Σ*± /Λ.

Short-lived resonances are used to measure the hadronic phase lifetime: 4–7 fm/c (PLB 802 (2020) 135225) in the most central collisions, in agreement with femtoscopic measurements.

Particle yield ratios

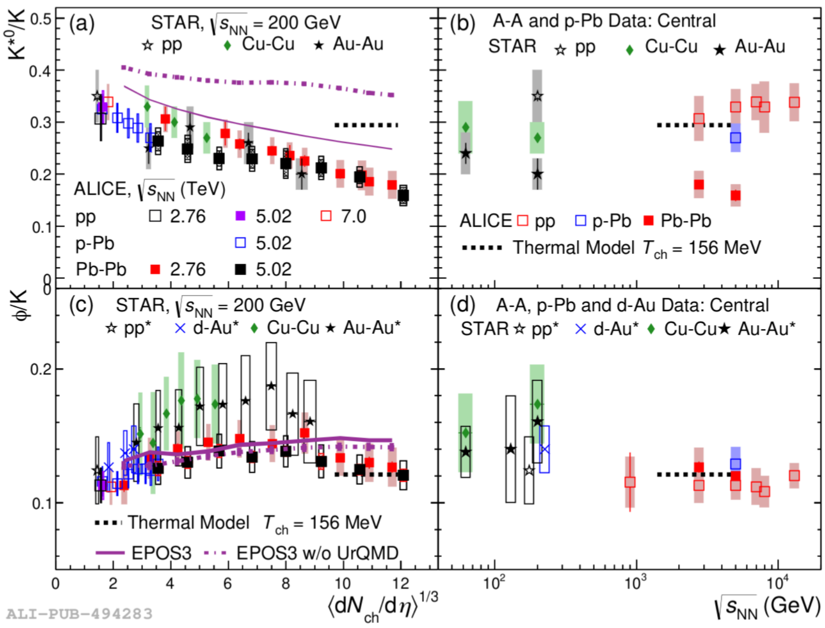

arXiv:2106.13113

K*/K:

Gradual decrease with the system size→effect of rescattering.
Lower values for Au–Au and Pb–Pb central collisions in all centre-of-mass energies.

ϕ/K:

approximately constant with the **system size (due to the larger lifetime)** and **centre-of-mass energies.**

- The **thermal** model predictions **without rescattering** effects agree with the ϕ/K and the K*/K in **small** systems, **but**

  K*/K in **central Pb–Pb** collisions is **not described**.

- **EPOS3 with UrQMD afterburner** (Phys. Rev. C 93 (2016) 014911) describes better the two ratios.

Particle yield ratios

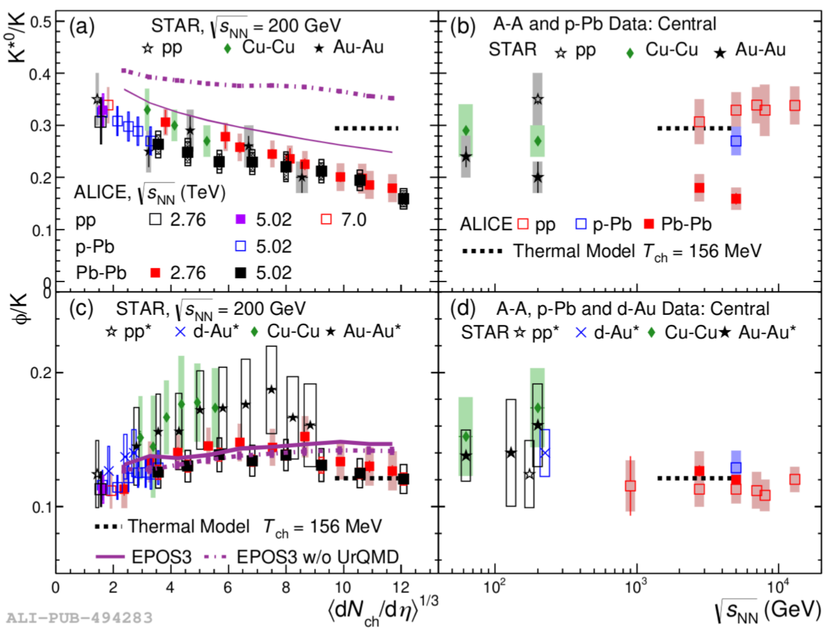

arXiv:2106.13113

K*/K:

Gradual decrease with the system size→effect of rescattering.

K*/K ratio slightly decreasing with multiplicity in pp and p–Pb → hint of non-zero lifetime of hadronic phase in small systems.

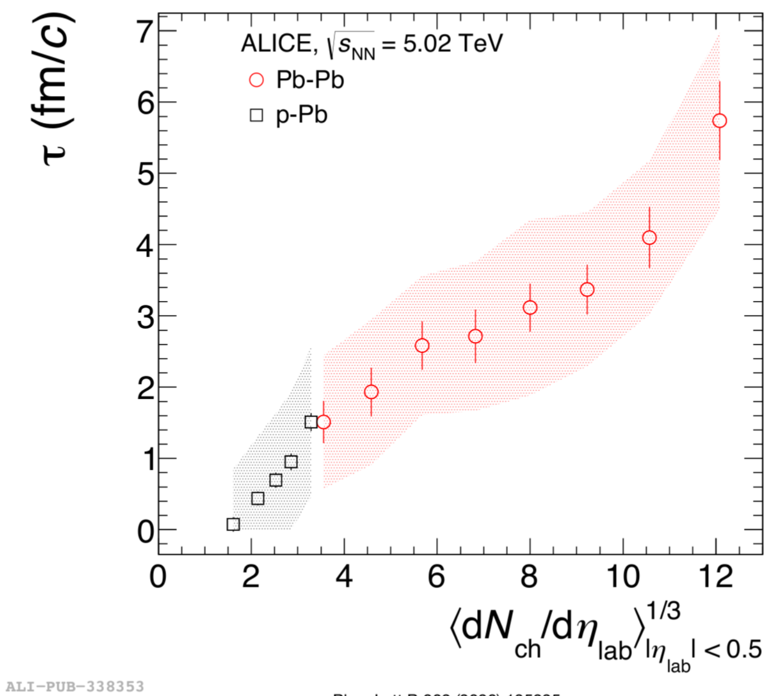

Phys.Lett.B 802 (2020) 135225

$$[\frac{K^{*0}}{K}]_{kinetic(Pb-Pb)} = [\frac{K^{*0}}{K}]_{chemical(pp)} \times exp(-\tau/\tau_K^{*0})$$

τ_K^{*0} = Lifetime of K^{*0}

τ : timespan between chemical and kinetic freeze-out.

Lower limit of the hadronic phase by studying the behaviour of $K^*(892)^0$. Assume no regeneration effects.

p_T differential yield ratios

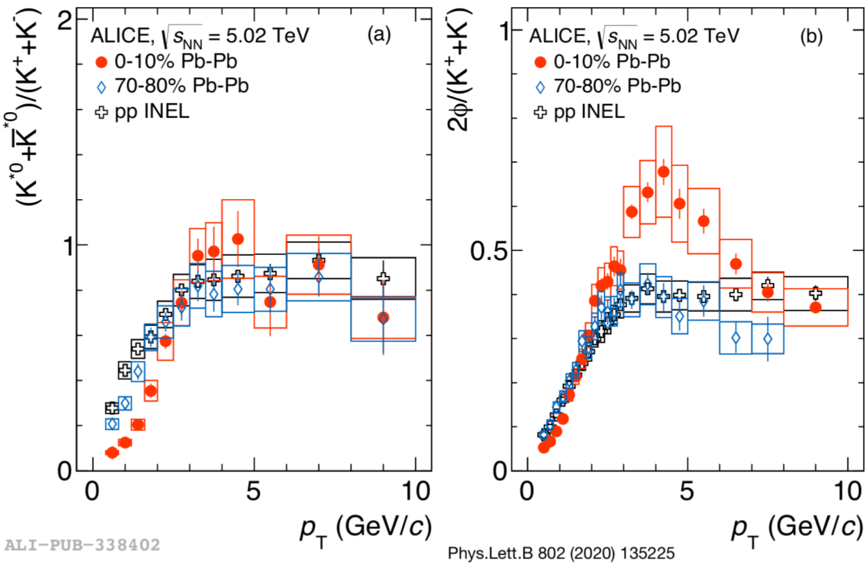

Phys.Lett.B 802 (2020) 135225

Low p_T: K^{*0}/K for central collisions are lower than peripheral (pp) collisions whereas ϕ/K are comparable within the uncertainties

- K^{*0} yields in central Pb–Pb collisions are suppressed due to re-scattering in the hadronic phase

- most effect on low momentum particles

Intermediate p_T: ratios show greater enhancement for central Pb–Pb collisions than peripheral and pp collisions

Particle yield ratios - ϕ meson

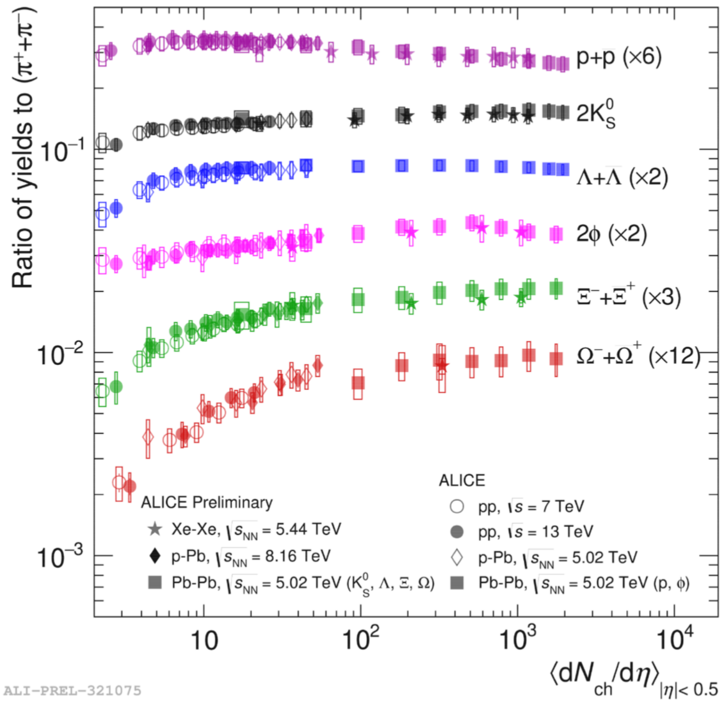

Smooth evolution with charged particle multiplicity in all available collision energies and systems (pp, p–Pb, Pb–Pb, Xe–Xe).

Strangeness **enhancement** increases with **strangeness content**.

ϕ: hidden strangeness. How does it behave?

Particle yield ratios - ϕ meson

ϕ/π: (ISI=0)/(ISI=0)

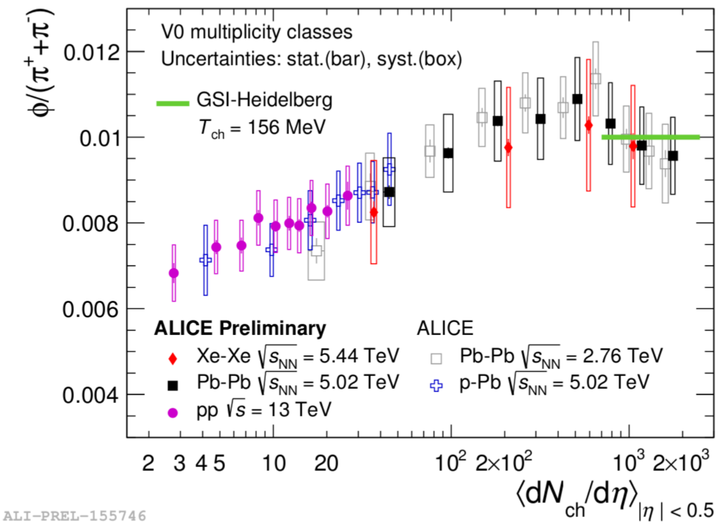

ϕ/π ratio saturates in Pb–Pb collisions and is consistent with thermal model predictions.

ϕ/π ratio increases with multiplicity in small systems, this is not expected for canonical suppression (see next slide).

Particle yield ratios - ϕ meson

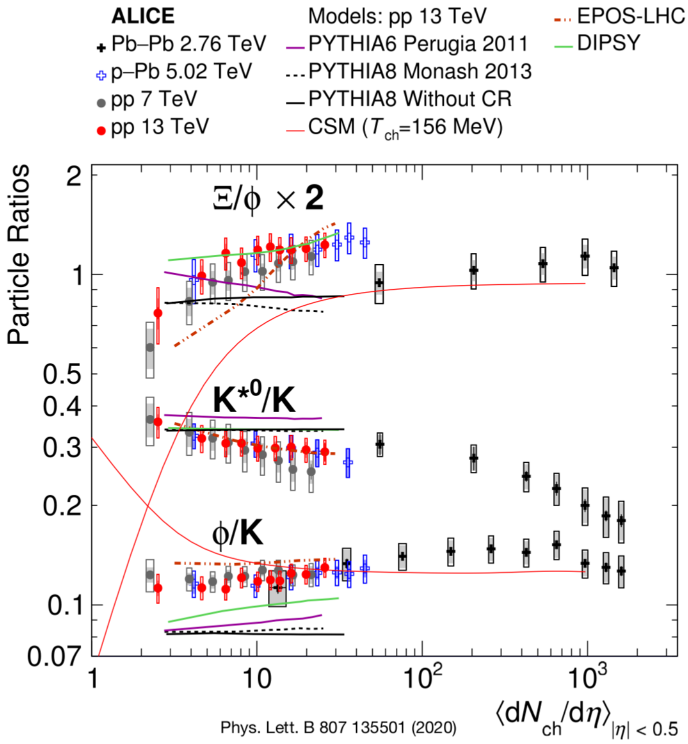

Phys. Lett. B 807 135501 (2020)

ALI-PUB-339048

ϕ/K (|S|=0)/(|S|=1)

flat or slightly increasing ratio at lowest multiplicities → suggests that ϕ behaves like a S ≧ 1 particle.

Ξ/ϕ (|S|=2)/(|S|=0)

- increases at low multiplicity.

- remains fairly flat across wide multiplicity range.

The ϕ has "effective strangeness" of 1–2 units.

Nuclear modification factors (R_{AA})

p_T distribution in A–A collisions

$$R_{AA} = \frac{dN_{AA} / dp_T}{\langle N_{coll} \rangle dN_{pp} / dp_T}$$

p_T distribution in pp collisions

Number of binary collisions, N_{coll}.

Nuclear modification factors (R_{AA})

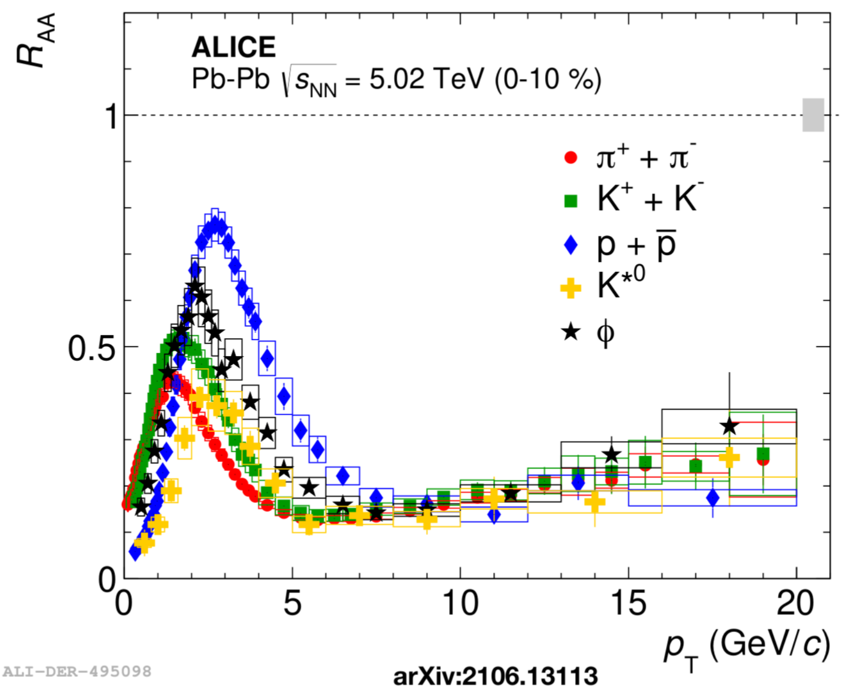

arXiv:2106.13113

p_T* < 2 GeV/*c:
K* ***R_{AA}*** values are **the smallest →**
Effect of re-scattering.

2 < *p_T* < 8 GeV/*c*:
- hadron mass dependence for mesons.
- Protons have the highest values of *R_{AA}*→ baryon-meson ordering.

***p_T* > 8 GeV/*c*: similar *R_{AA}* values** for all **hadron species** within the uncertainties →
the relative particle composition at high *p_T* remains the same as in vacuum.

Exploring new resonances: Ξ(1820)

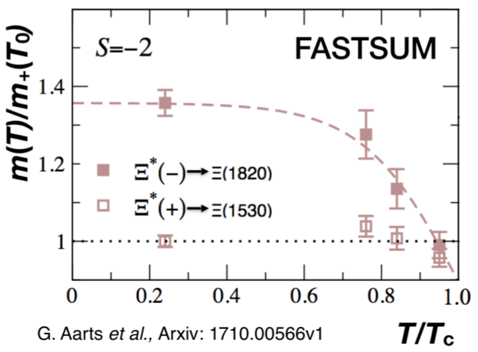

G. Aarts *et al.*, Arxiv: 1710.00566v1

FASTSUM collaboration:
(lattice QCD simulations)

In the presence of unbroken chiral symmetry, it can be shown that positive- and negative-parity baryonic channels are degenerate, and hence there is parity doubling.

Expected signal experimentally:
mass shift, width broadening or change in yield ratio between Ξ(1820) and Ξ(1530).

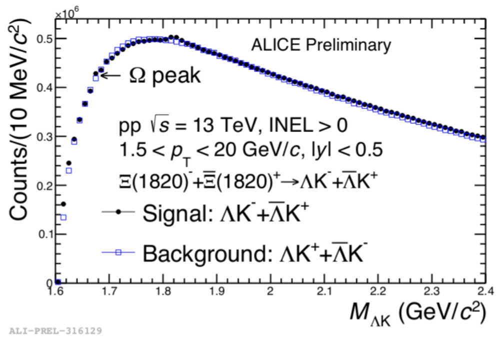

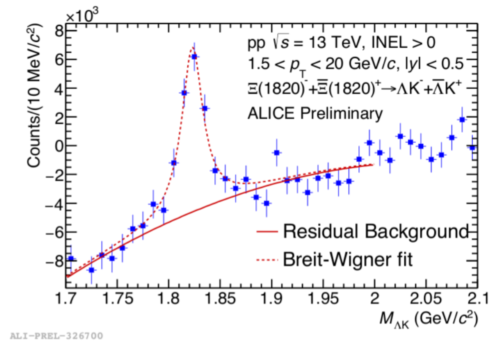

Exploring new resonances: $f_0(980)$

Quark contents of $f_0(980)$ is still controversial.

Study of $f_0(980)$ production would give a hint of its quark contents → tetraquark candidate.

On-going effort in all available collision systems.

Reconstructed via $f_0(980) \to \pi^+ \pi^-$

Large contributions from other resonances.

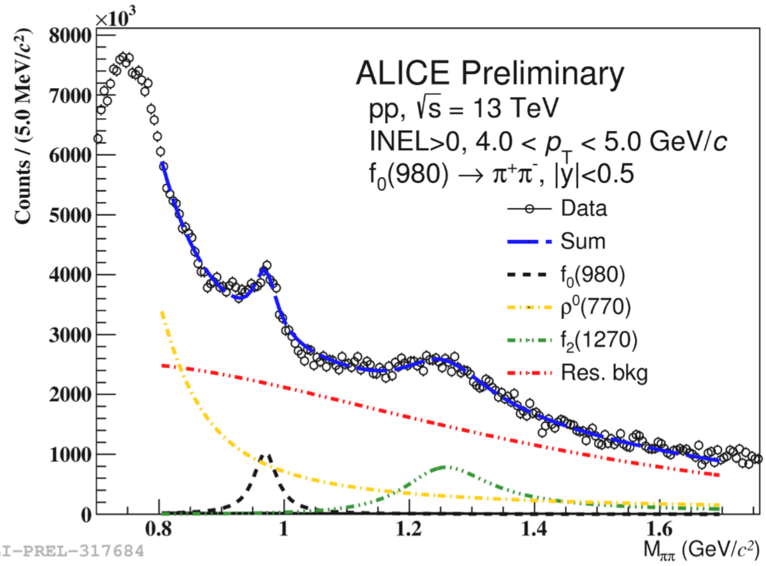

The future…

- More statistics accumulated in the forthcoming runs will result in more precision measurements.
- This will enable also multi-differential analyses, for example:

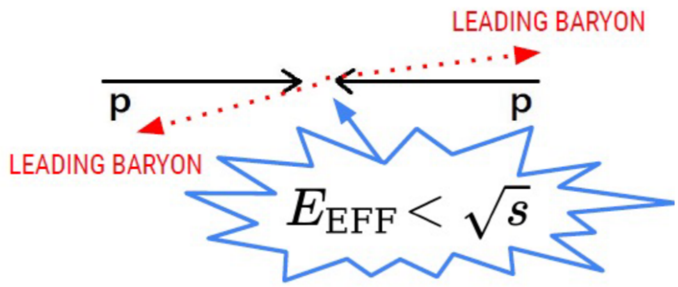

Dependence of strangeness production on effective energy.

The future…

- More statistics accumulated in the forthcoming runs will result in more precision measurements.
- This will enable also multi-differential analyses, for example:

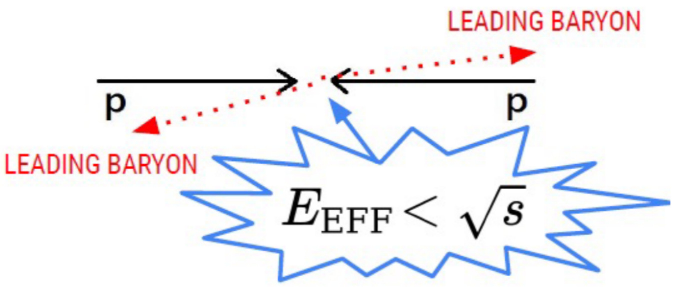

Dependence of resonance production on effective energy.

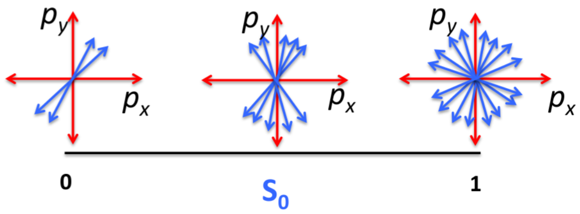

$$S_o = \frac{\pi^2}{4} \min_{\hat{n}=(n_x,n_y,0)} \left(\frac{\sum_i |\vec{p}_{Ti} \times \hat{n}|}{\sum_i p_{Ti}} \right)^2$$

$$S_0 = \begin{cases} 0 & \text{“pencil-like” limit (hard events)} \\ 1 & \text{“isotropic” limit (soft events)} \end{cases}$$

Dependence of resonance production on event topology.

Summary

ALICE has provided a comprehensive study of resonances in pp, p-Pb and Pb-Pb collisions at various energies with very interesting results.

- **Parton** energy **loss** at high p_T is **species independent**.

- The **hardening of p_T spectra** is observed in **small** collision **systems → collective flow-like phenomena in small systems**.

- **Resonance** production is **independent** of the collision **energy** and **system** and it is **driven** by the event **multiplicity**.

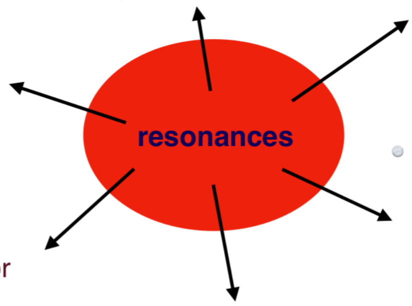

- **ρ^0, K^{*0}, $\Sigma^{*\pm}$, Λ^* are suppressed** in **most central** collisions with respect to small collisions systems.
  ϕ with τ = 46.4 fm/c is **not suppressed**. It has an effective **strangeness of 1-2** units.

- **Rescattering** is the **dominant** process in the hadronic phase for short-lived resonances (τ < ~15 fm/c).

- More resonances are being explored: **$f_0(980)$ and $\Xi(1820)$**.

Backup

Models

The **EPOS3** model describes the evolution of a heavy-ion collision with the reaction volume being divided into a core and a corona part. After hadronization, hadrons are fed into the UrQMD hadron cascade afterburner, which describes hadronic interactions in a microscopic approach.

- H. J. Drescher, M. Hladik, S. Ostapchenko, T. Pierog, and K. Werner, "Parton based Gribov-Regge theory", Phys. Rept. 350 (2001) 93–289, arXiv:hep-ph/0007198.
- K. Werner, I. Karpenko, T. Pierog, M. Bleicher, and K. Mikhailov, "Event-by-Event Simulation of the Three-Dimensional Hydrodynamic Evolution from Flux Tube Initial Conditions in Ultrarelativistic Heavy Ion Collisions", Phys. Rev. C 82 (2010) 044904, arXiv:1004.0805 [nucl-th].

The **statistical hadronization model** describes the process of hadron formation at the scale where QCD is no longer applicable. It is assumed that near hadronization the fireball created in heavy-ion collisions is close to thermal equilibrium and hadron yields can be characterized by a grand canonical partition function.

- A. Andronic, P. Braun-Munzinger, K. Redlich, and J. Stachel, "Decoding the phase structure of QCD via particle production at high energy", Nature 561 no. 7723, (2018) 321–330, arXiv:1710.09425 [nucl-th].